Journal of
Materials Chemistry B

Materials for biology and medicine

Accepted Manuscript

This article can be cited before page numbers have been issued, to do this please use: Z. Zhao, H. Yang, W. Zhao, S. Deng, K. Zhang, R. Deng, Q. He, H. Gao and J. Li, *J. Mater. Chem. B*, 2020, DOI: 10.1039/C9TB02388G.

ROYAL SOCIETY OF CHEMISTRY

rsc.li/materials-b

View Article Online
DOI: 10.1039/C9TB02388G

Graphene-nucleic acid biointerface engineered biosensors with tunable dynamic range

Zhifeng Zhao,‡ [ab] Hao Yang,‡ [ab] Wenyue Zhao,[a] Sha Deng,[a] Kaixiang Zhang,[bc] Ruijie Deng,*[a] Qiang He,[a] Hong Gao[a] and Jinghong Li*[b]

[a] *College of Biomass Science and Engineering, Healthy Food Evaluation Research Center, Sichuan University, Chengdu 610065, China*

[b] *Department of Chemistry, Key Laboratory of Bioorganic Phosphorus Chemistry & Chemical Biology, Tsinghua University, Beijing 100084, China*

[c] *School of Pharmaceutical Sciences, Zhengzhou University, Zhengzhou 450001, China*

‡ These authors contributed equally to this work.

*E-mail: jhli@mail.tsinghua.edu.cn; drj17@scu.edu.cn

View Article Online
DOI: 10.1039/C9TB02388G

ABSTRACT: Programmed biosensors with tunable quantification range and sensitivity would greatly broaden their application in medical diagnosis, food safety and environmental analysis. Herein, we proposed a graphene-nucleic acid biointerface engineered biosensor, allowing to detect target molecules with adjustable dynamic ranges and sensitivities. The biosensors were programmed by simply tuning the poly A tail of aptamer probes. The tuning of the poly A tail would allow to modulate the interaction between aptamer probes and graphene oxides (GO), in turn programing the competitive binding processes of aptamer probes to target molecules and GO. The biosensors, termed **a**ffinity-**t**unable **aptasensors** (atAptasensor) could be easily tuned with different dynamic ranges by using aptamer probes with different tail lengths, and the dynamic range could be extended to be over 3 orders by a combination use of multiple aptamer probes. Remarkably, the specificity of aptamer probes would be increased by increasing the interaction between aptamer probes and GO. Reliability of atAptasensor for ATP detection was testified in serum and milk samples, and we also applied atAptasensor for culture-independent analysis of microorganism pollution.

KEYWORDS: aptamer; graphene; microorganism; ATP; biosensors

View Article Online
DOI: 10.1039/C9TB02388G

1. Introduction

Over the past decade, enormous biosensors based on RNA and DNA aptamers (termed aptasensors) have emerged.[1,2] Aptamers serve as highly specific recognition component, and confer aptasensors with high selectivity and affinity for target molecules.[3-5] By integration with different nanomaterials such as graphene and gold nanoparticles,[6] highly efficient and cost-effective sensing platforms have been constructed to detect target molecules ranging from heavy metal,[7] small molecules,[8-12] proteins[13,14] to pathogens[15] and mammal cells.[16] Nevertheless, great efforts focus on improving the sensitivity of biosensors,[17-19] always ignoring their dynamic sensing range. The quantification range of biosensors plays equally important role in practical applications. For example, the monitoring for viral loading requires a corresponding biosensor with tunable dynamic range because the virus concentration may vary over numerous orders of magnitude. In general, ultrasensitive biosensors with fixed dynamic range are not able to detect the samples in high end of the concentration range. Herein, we proposed a graphene-nucleic acid biointerface engineered aptasensors, and allow to detect target molecules with tunable dynamic ranges by simply adjusting the 3'-tailing nucleotides of aptamer sequences.

In order to construct a biosensor with tunable dynamic range, a set of receptor variants should be designed to manifest similar specificity but different target affinity.[20] Several works have demonstrated that DNA probes could be programmed to be tunable receptors.[21,22] By designing molecule beacons with different stem lengths[22] or double stranded-DNA probes with mutated bases,[23] aptasensors could be built with

View Article Online
DOI: 10.1039/C9TB02388G

editable dynamic ranges. However, the stability of DNA probe structures needs to be elaborately designed, while it still could hardly be precisely predicted, thus iterative sequence-based optimization is demanded.

Besides the structural design of DNA probes, nanomaterial-nucleic acid biointerface may potentially be engineered by designing the sequences of DNA/RNA probes,[24] conferring adjustable interaction between nanomaterials and DNA/RNA probes. The engineered nanomaterial-nucleic acid biointerface can be potentially utilized to modulate the dynamic range of aptasensor, and still has not been well explored. DNA with different nucleotide components (A, T, C and G) or sequences would present different affinity toward inorganic nanomaterials including carbon nanomaterials, metal nanoparticles and metal oxides.[24] Graphene oxide (GO) has drawn considerable interest on account of its unique mechanical properties, biocompatibility, large surface area for adsorbing single-strand DNA, and fluorescence quenching efficiency.[25,26] We and other groups have systematically studied the interaction between graphene and DNA probes,[27-29] and have constructed a series of biosensors to detect small molecules,[30-32] DNA sequences,[33] mRNAs,[34,35] proteins,[36] and kinase.[37]

Herein, we explored the engineering of graphene-nucleic acid biointerface for constructing dynamic range tunable aptasensors. We fabricated a set of length-altered aptamer probes by the utilization of the modulated affinity of poly A sequences. Aptamer probes with different 3'-terminal tailing A sequences have been designed to construct the biosensors with programmable dynamic range. A broad dynamic range could be achieved by the incorporation of multiple aptamer probes. Based on the

View Article Online
DOI: 10.1039/C9TB02388G

programmable aptasensors, we could precisely detect ATP ranging from 2 μM to 3500 μM (over 3 orders). Furthermore, all the aptasensors generated by this strategy were verified to be specific to ATP, and allowed for one-pot, homogeneous detection of ATP at room temperature. The aptasensors, termed **a**ffinity-**t**unable **aptasensors** (atAptasensor) were applied to detect ATP in serum and milk samples, as well as *Escherichia coli* (*E. coli.*) pollution.

2. Experimental section

2.1 Materials and reagents

GO was synthesized based on a modified Hummers' method according to our published work.[30] Adenosine triphosphate (ATP), cytidine triphosphate (CTP), guanosine triphosphate (GTP), uridine triphosphate (UTP), adenosine, adenosine monophosphate (AMP), adenosine diphosphate (ADP), glutathione (GSH), and serum were purchased from Sigma-Aldrich (St. Louis, MO, USA). The milk was bought from the local supermarket. *Escherichia coli* (*E. coli.*) *(ATCC 43889)* was a laboratory preservation strain. All DNA oligonucleotides (Table S1, ESI), synthesized by Sangon (Shanghai, China), and were HPLC purified. The DNA oligonucleotides were modified with 6-carboxyfluorescein (FAM) fluorophores at the 5' terminal.

2.2 Characterization of GO and GO/aptamer probes

The AFM images of pristine GO and GO/aptamer probes were collected using a multimode atomic force microscope (AFM) under tapping mode (SmartSPM, AIST-NT, USA) using a mica plate. The samples were also observed by a high-resolution transmission electron microscope (HT7700, Hitachi, Japan) with an

View Article Online
DOI: 10.1039/C9TB02388G

accelerating voltage of 100 kV. The Raman observation for GO was conducted on a Horiba-Jobin-Yvon Raman system (laser wavelength 514 nm, power 0.5 mW).

2.2 Detection procedures

The detection process was carried out in a volume of 35 μL containing 3.5 μL 10×binding buffer (330 mM Tris-HCl (pH 7.9 at 25 ℃), 100 mM $MgCl_2$, 660 mM KCl), 3.5 μL FAM-labeled aptamer probes (1.5 μM), 3.5 μL ATP solution at various concentrations and 21.5 μL H_2O. Afterwards, the mixture was incubated for 20 min at room temperature to complete the binding of aptamers toward ATP. Then, 3.5 μL GO suspension (250 μg/mL) was added into the solution and incubated for 10 min at room temperature to quench the fluorescence of aptamer probes, and followed by fluorescence measurement. All reactions were carried out in triplicate and data were presented as means ± relative standard deviation (RSD).

2.3 Fluorescence and real-time fluorescence measurements

For the fluorescence spectra analysis, a fluorescence microplate reader Synergy H1 (BioTek, USA) was used to record the emission spectra of 510-650 nm at 480 nm of excitation wavelength. Real-time fluorescence analysis was carried out at the emission of 522 nm with the excitation of 480 nm using 50 μL volume of mixture with the same concentrations as that used for ATP detection.

2.4 Application of ATP detection in complex samples

To exclude interferential biomolecules in sample matrix, pretreatment including centrifugation, filtration and dilution process was involved. 100 μL of samples (serum and milk) were added in a 200 μL centrifuge tube, and then centrifuge at 8000 rpm for

View Article Online
DOI: 10.1039/C9TB02388G

5 min at room temperature to obtain a supernatant. The supernatant was diluted 10 times with H_2O. Then the diluent was filtered by a syringe filter made of polyether sulfone (0.22 μm) . ATP with various concentrations was added to prepare the real sample solution, and the detection process was proceeded according to the above procedures.

2.5 Application of *E. coli.* detection

For bacterial detection, *E. coli.* was chosen as the model. *E. coli.* was cultivated for 12 h in sterile Nutrient Broth (NB) (1.0 g peptone, 0.5 g sodium chloride and 0.3 g beef extract powder dissolving in 100 mL H_2O), and continuously oscillated at 37 ℃. Then, cultured solution was sterilized at 121 ℃ for 20 min, accompanied by the dissolution of cellular contents. Next, the bacteria solution was filtered by a syringe filter (0.22 μm), and the filtrates were then analyzed by the procedures described above.

3. Results and discussion

3.1 Working principles

Nucleic acid sequences with different lengths have been manifested to be presented with tunable binding force to GO surfaces, thus allowing to be used to engineer the biointerface of nucleic acid/GO. We constructed an **a**ffinity-**t**unable **aptasensor** (termed atAptasensor) by programming nucleic acids/GO biointerface. atAptasensor was performed using an aptamer probe compromised with two modules: recognition domain and affinity domain (Fig. 1). Recognition domain was a fluorophore-labeled aptamer sequence that specifically identified target molecules. And affinity domain was a binding sequence, and endowed the aptamer probes with adjustable binding

View Article Online
DOI: 10.1039/C9TB02388G

affinity toward GO surfaces. Recognition domain could function as the general working principle of GO/aptamer probes. The binding of target molecules toward aptamers would sustain a structure-switching process of aptamer sequences, generally weaken the binding ability of aptamer probes to GO surfaces. Sequentially, the detachment of aptamer probes from GO surfaces would turn on the fluorescence. DNA sequences with polynucleotide tail could strengthen the affinity between DNA with GO and scarcely affected the ability of recognition domain[24,38] (increasing the poly A tail did not significantly change the conformation of ATP aptamer, Fig. S1, ESI). In principle, the binding affinity of aptamer probes could be finely tuned by its sequence. Besides the binding of aptamer sequences, an extra sequence of poly A at the tail of the probe would allow to program the affinity of aptamer probes to GO surfaces. The increase of the length of the tailing sequences would endow a higher affinity of aptamer probes toward GO, and allow to modulate the competing process between GO binding and target binding. The adjustable binding affinity of aptamer probes toward GO would in turn result in a tunable dynamic range of atAptasensor. Elaborately tuning of the quantification range as well as the limit of detection (LOD) of atAptasensor could be achieved by simply changing the tail length of aptamer probes, no complex probe design was involved. Besides, by simultaneously using aptamer probes with different affinities, we could extend the broad dynamic range of aptasensors, thus allow to precisely detect target molecules with orders of concentrations.

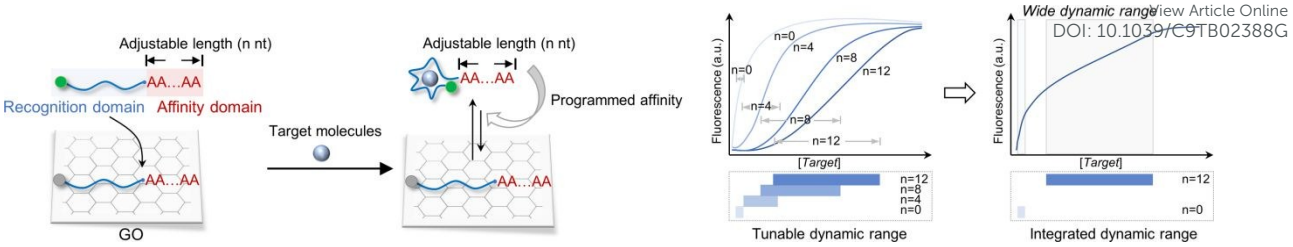

Fig. 1 Schematic representation of working principles of atAptasensor. The aptamer probes contain recognition domain (fluorophore-labeled aptamer) and affinity domain (poly A sequences). The affinity of aptamer probes toward GO could be finely tuned by adjusting the length of affinity domain, in turn to control the competitive binding of target molecule binding and GO binding. The dynamic range of atAptasensor could be tuned by using aptamer probes with different lengths of poly A tail or extended by a combined use of different aptamer probes.

Firstly, GO was synthesized, and the response of GO/aptamer probes toward target molecules was tested. As shown in Fig. 2A, GO nanosheets were obtained by a modified Hummers' method. The GO nanosheets had a typical thickness (~1 nm) of single-layer GO sheets (Fig. 2B and 2C). The Raman spectra of GO presented the existence of the two characteristic peaks of the D band and G band of GO (Fig. 2D), further confirmed the successful synthesis of GO sheets. Initially, a FAM-labeled aptamer probe without the incorporation of poly A tail (termed T0A) was used to test the response of GO/aptamer probes, and ATP was chosen as the target molecule (Fig. 2E). The addition of GO would almost totally quench the fluorescence of T0A. A majority of the fluorescence would be recovered in the presence of ATP (3 mM), resulting in a signal-to-background ratio of up to be 104. The high

View Article Online
DOI: 10.1039/C9TB02388G

signal-to-background ratio of GO/aptamer probes toward target molecules would accommodate the engineering of precisely controlled aptasensors.

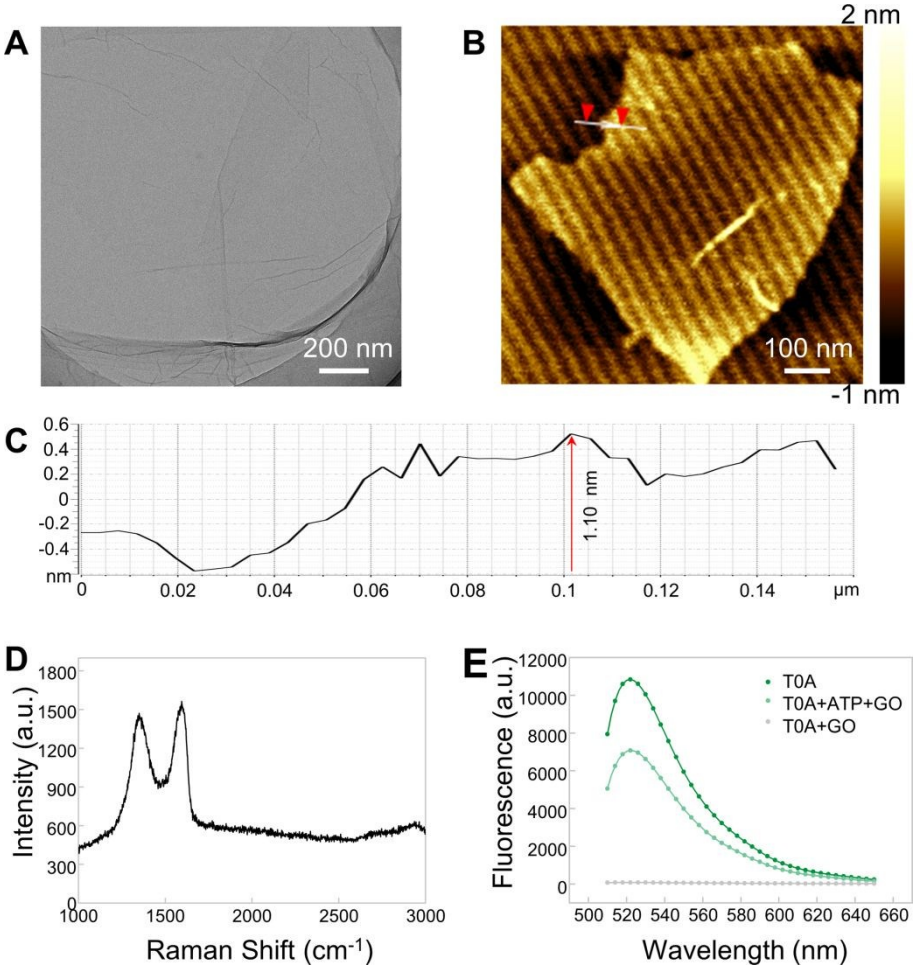

Fig. 2 Characterization of GO and GO/aptamer probes. (A) A typical TEM image of GO; (B) AFM image of GO; (C) The thickness of measured GO; (D) Raman spectra of GO; (E) Fluorescence response of aptamer probes in the presence or absence of GO and ATP.

We set to explore the engineering of the interaction between aptamer probes and GO, and construct 4 aptamer probes with different poly A tails. Probes T0A, T4A, T8A and T12A were with 0 nucleotide (nt), 4 nt, 8 nt and 12 nt A nucleotides. We

View Article Online
DOI: 10.1039/C9TB02388G

tested the morphology changes in the GO induced by functionalization with aptamers of different lengths by the utilization of AFM (Fig. S2, ESI). The average thickness of GO nanosheets had a tiny increase by functionalization with aptamers of longer lengths, indicating the successful binding of aptamer probes on GO surface. All of these GO/aptamer probes could be efficiently response to target molecules as their fluorescence would significantly turn on in the presence of ATP (Fig. 3A). Specifically, lengthening the poly A tail would contribute to a lower fluorescence both in the absence or presence of ATP, especially the number of A nucleotides turned from 0 nt to 8 nt. The signal to background ratio would change from 93 to 61 when the length of poly A increased from 0 to 8 nt (Fig. 3B). The increase of the length of the polynucleotide tail would improve the binding affinity of aptamer probes towards GO，[24,29], competitively reducing the affinity of target molecules ATP towards GO/aptamer probes and the possibility of the leave of aptamer probes from GO surfaces. The principle based on the turning of the affinity of target molecules towards nucleic acid probes has been applied to construct biosensors with tunable dynamic range.[22, 23] We aimed to turning the dynamic range of biosensors by engineering the interaction between nanosurface and nucleic acid probes. The response of GO/aptamer probes toward target molecules could be efficiently tuned by changing the length of poly A tails. A further increase of length of poly A tail from 8 nt to 12 nt only led to a tiny decrease of fluorescence. Thus, aptamer probes of a length of poly A tail over 12 nt were not tested.

View Article Online
DOI: 10.1039/C9TB02388G

Further, we tested the effect of poly A tails on the kinetic of the binding processes of aptamer probes. The fluorescence would remain to be stable within 10 min starting from the addition of T0A (Fig. S3, ESI). While for T12A, a shorter time of about 5 min was needed to allow aptamer probes to stably bind on GO surfaces. The binding of aptamer probes toward GO would be finished upon the addition of ATP and T12A, indicating the fast binding kinetic of T12A. And it would take about 10 min for T0A to stably interact with GO in the presence of ATP. The result further reveals that a longer poly A tail would confer a higher affinity of aptamer probes, thus facilitate their binding to GO surfaces.

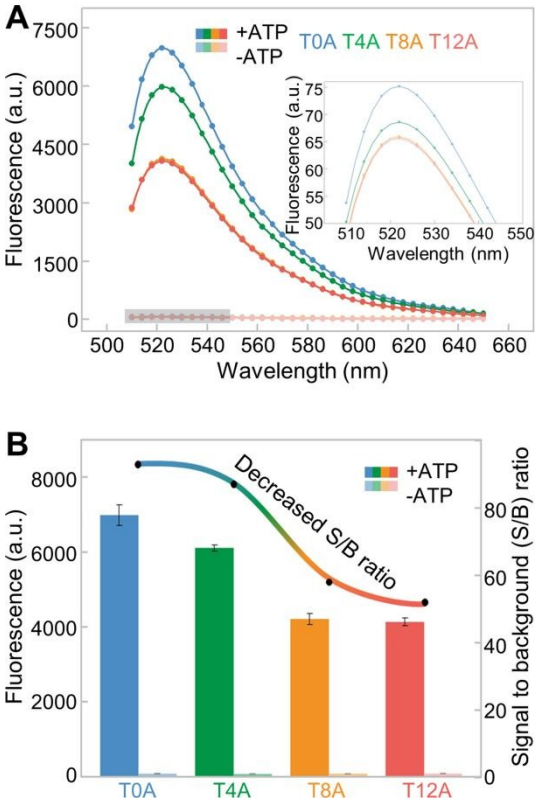

Fig. 3 Fluorescence response of atAptasensor using aptamer probes with different poly A tails toward ATP. (A) Fluorescence curves corresponding to atAptasensor using

View Article Online
DOI: 10.1039/C9TB02388G

different aptamer probes (T0A, T4A, T8A and T12A) in the presence or absence of ATP; (B) Fluorescence intensity of atAptasensor using different aptamer probes corresponding to (A) and the obtained signal-to-background ratio. The excitation wavelength was set at 480 nm, the concentrations of ATP, GO and aptamer probes were 2 mM, 25 μg/mL and 150 nM, respectively.

To investigate the feasibility of the utilization of biointerface design for engineering aptasensors, we tested the quantification performance of aptamer probes, T0A, T4A, T8A and T12A. Firstly, we optimized the concentration of GO to obtain the maximal response of aptamer probes toward ATP (Fig. S4, ESI). We then tested the fluorescence responses of 4 aptamer probes toward ATP with concentrations ranging from 0 to 6000 μM (Fig. 4 and Fig. S5, ESI). All of these aptamer probes would contribute to a dramatically increased fluorescence with the addition of ATP in low-concentration range, however, presented a small response at high end concentration of ATP. This may be due to the saturated binding of ATP toward aptamer probes. The linear dose-response ranges using T0A, T4A, T8A and T12A were 2~500 μM, 10~1000 μM, 50~2500 μM and 750~3500 μM, respectively. Further, we estimated the sensitivity of these aptamer probes. The limit of detection (LOD) of aptasensors was defined as the ATP concentration corresponding to the fluorescence intensity 3 times of the standard deviation higher than the background signal. The LOD of aptasensors using T0A, T4A, T8A and T12A were calculated to be 1.07 μM, 22.22 μM, 42.05 μM and 760.2 μM, respectively. Obviously, the tuning of poly A tails would significantly influence the responses of aptamer probes toward ATP at different

View Article Online
DOI: 10.1039/C9TB02388G

concentrations. This result confirms that the engineering of biointerface of aptamer probes/GO could efficiently tune the detection performances of aptasensors. Increasing the length of poly A tail would enhance the interaction between aptamer probes and GO, in turn resisting the binding of ATP molecules. Thus, aptamer probes with longer poly A tail could efficiently response to ATP in a relatively higher concentration, and led to a higher LOD. However, the higher affinity between aptamer probes and GO would accommodate the aptasensors for detecting ATP in higher concentrations. For example, aptasensors could broaden the maximal detection concentration of ATP from 500 μM to 3500 μM by using T12A instead of T0A. Simply change of the length of poly A tail could efficiently engineer the biointerface of nucleic acids/GO, and allow to elaborately tuning the quantification range of aptasensor.

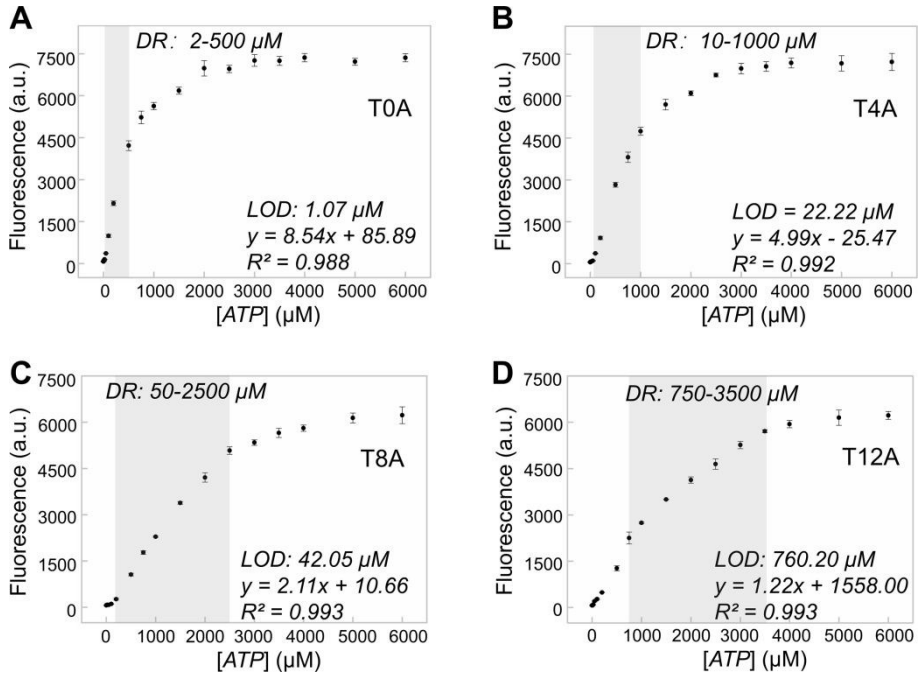

Fig. 4 The plot of fluorescence signal for atAptasensor using T0A (A), T4A (B), T8A (C) and T12A (D) with respect to the concentration of ATP. The excitation wavelength

View Article Online
DOI: 10.1039/C9TB02388G

was set at 480 nm, and the emission wavelength was 522 nm. The concentrations of GO and aptamer probes were 25 μg/mL and 150 nM, respectively.

We then explored the potential of atAptasensor for broad-range detection of target molecules by coalesced use of multiple aptamer probes. For simplicity, aptamer probes were used in equimolar concentrations except for the 4-component constituted atAptasensor. 4 species of atAptasensor, T0A, T0A/T8A (1:1), T0A/T12A (1:1) and T0A/T4A/T8A/T12A (1:3:3:3) (the content ratio was defined as molar concentrations) were tested (Fig. S6, ESI). atAptasensor with 2 components of aptamer probes (T0A/T8A (1:1) and T0A/T12A (1:1)) could generate two continuous linear dose-response parts (Fig. 5B and 5C). For T0A/T8A (1:1), the linear dynamic range was 10-500 μM and 500-2000 μM. Compared to atAptasensor using 100% T0A (Fig. 5A), atAptasensor with an extra addition of T8A would result in a higher LOD (10 μM). This may be because T8A would competitively sequester parts of ATP molecules.[20, 22] T8A endowed a lower sensitivity to ATP detection (Fig. 4A and 4C) compared to T0A, thus atAptasensor using T0A/T8A (1:1) led to a reduced response toward ATP in low concentration. Nevertheless, the addition of T12A would not significantly affect the sensitivity of atAptasensor. This may be because GO/T12A would present a dramatically higher affinity between GO and aptamer probes compared to GO/T0A, thus ATP were preferentially binding with T0A probe rather than T12A. Thus, the addition of a longer poly A tailed aptamer probe (T12A) would not significantly influence the binding process of ATP toward T0A. Further, we tested a 4-component aptamer probe T0A/T4A/T8A/T12A (1:3:3:3), a dynamic range of over 3-order (2-3500 μM) could be achieved (Fig. 5D, Table S2, ESI).

View Article Online
DOI: 10.1039/C9TB02388G

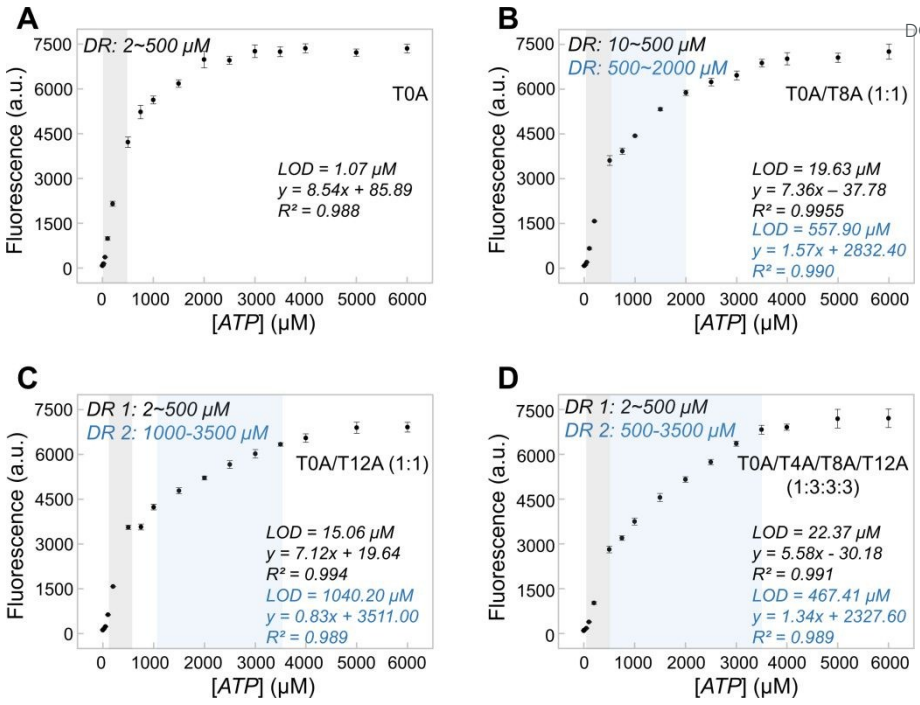

Fig. 5 The plot of fluorescence signal for atAptasensor using T0A (A), T0A/T8A (1:1) (B), T0A/T12A (1:1) (C), and T0A/T4A/T8A/T12A (1:3:3:3) (D) (the content ratio was defined as molar concentrations) with respect to the concentration of ATP. The excitation wavelength was set at 480 nm, and the emission wavelength was 522 nm. The concentration of GO was 25 μg/mL. The concentrations of aptamer probes were 150 nM (including all component of aptamer probes).

3.2 Selectivity evaluation

To assess the selectivity of atAptasensor for ATP detection, the response of constructed atAptasensor toward other nucleotide species including GTP, CTP and UTP was evaluated under the same experimental conditions as for ATP detection (Fig. 6). The final concentration of the analytes was all 3 mM. For all atAptasensors using the single-component aptamer probes (T0A, T4A, T8A, and T12A), and multi-component aptamer probes (T0A/T8A (1:1), T0A/T12A (1:1), and

View Article Online
DOI: 10.1039/C9TB02388G

T0A/T4A/T8A/T12A (1:3:3:3)), the binding and response toward other analytes (GTP, CTP, and UTP) were barely proceeded since tiny fluorescence intensity were observed after the addition of those analytes into the system. We defined the discrimination factor (DF) as the ratio of the fluorescence of aptamer probes with the addition of ATP to other non-target molecules. The DFs for GTP discrimination using T0A, T4A, T8A and T12A were 3.98, 5.25, 7.42 and 11.64, respectively, for CTP discrimination were 11.82, 37.36, 43.28 and 14.84, respectively, and for UTP discrimination were 16.28, 44.05, 49.12 and 15.45, respectively (Table S3, ESI). Particularly, the DFs for GTP, CTP and UTP would dramatically increase when the length of poly A changed from 0 nt to 8 nt (from T0A to T8A), indicating the incorporation of poly A tail would increase the selectivity of GO/aptamer probes. For T12A, the DFs for CTP and UTP would be reduced when compared to T8A. The reduced DF using T12A resulted from a higher background.[29] This result indicates that the engineering of the biointerface of nucleic acids/nanomaterials may be potentially be utilized to improve the specificity of aptamer probes by appropriately adjust the poly A tail. Nevertheless, we tested atAptasensor for discriminating adenosine, AMP, ADP, and ATP, and presented relatively poor specificity (Fig. S7, ESI). The chosen aptamer was demonstrated to exert relatively poor ability to discriminate adenosine, AMP and ADP from ATP,[40, 41] since there were only differences of phosphate groups between ATP and AMP/ADP/adenosine.

View Article Online
DOI: 10.1039/C9TB02388G

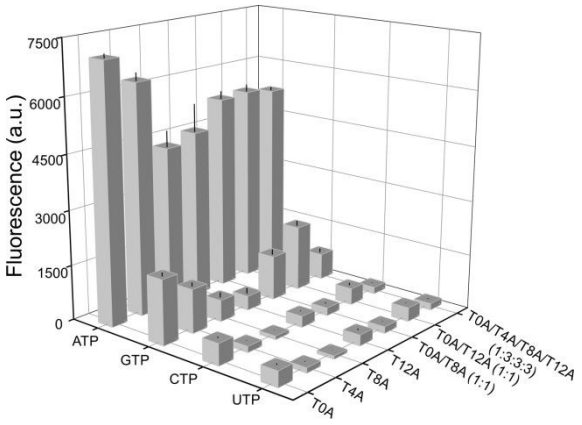

Fig. 6 Selectivity of atAptasensor for ATP detection using different aptamer probes or aptamer probe sets. The concentrations of ATP, GTP, CTP and UTP were all 2 mM. The concentration of GO was 25 μg/mL. The concentrations of aptamer probes were 150 nM (including all component of aptamer probes). All real samples were carried for 3 parallel tests.

3.3 Application ATP and microorganism detection

We finally tested the performance of atAptasensor for ATP and microorganism detection in complex samples. For ATP detection, serum and milk samples were chosen. ATP with concentrations ranging from 200 to 3000 μM were pre-added into the serum and milk samples. Aptamer probe, T0A/T12A (1:1) was used to detect ATP in serum and milk samples. The recovery rates of ATP detection in serum and milk ranged from 90.7% to 105.0%, and the relative standard deviation (RSD) was lower than 9.88% (Table 1 and Fig. S8, ESI). Thus, atAptasensor could allow to precisely detect ATP in different complex samples.

View Article Online
DOI: 10.1039/C9TB02388G

Table 1. Determination of ATP spiked in the serum and milk samples*

Samples	Added (μM)	Found (μM)	Recovery (%)	RSD (%) n=3
Serum	200	199	99.48	5.79
	1000	1050	105.00	9.88
	3000	2868	95.62	6.01
Milk	200	205	102.62	5.93
	1000	907	90.72	9.55
	3000	3079	102.65	5.99

* The conditions for ATP detection: the concentration of GO was 25 μg/mL. The concentrations of aptamer probes were 150 nM (75 nM T0A and 75 nM T12A). All real samples were carried for 3 parallel tests.

Furthermore, we applied atAptasensor to detect microorganism. As the concentration of ATP usually corresponds to the degree of microorganism contaminations, and ATP assays are often used to quantification the content of microorganism.[42] Aptamer probe, T0A/T4A/T8A/T12A (1:3:3:3) was used to detect *E. coli.*, and the number of *E. coli.* was quantified by plate counting method. The result showed that a good response between the fluorescence intensity and the concentration of *E. coli.* cells (with a R^2 of 0.988) using atAptasensor (Fig. 7), indicating the potential use of atAptasensor for detecting microorganism contaminations.

View Article Online
DOI: 10.1039/C9TB02388G

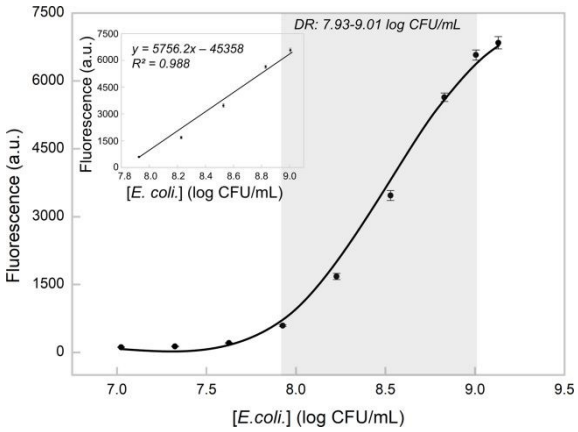

Fig. 7. The plot of fluorescence signal of atAptasensor with respect to the concentration of *E. coli.*. Inset: the linear range for determination of *E. coli.*. the concentration of GO was 25 μg/mL. The concentrations of aptamer probes were 150 nM (15 nM T0A, 45 nM T4A, 45 nM T8A and 45 nM T12A). All real samples were carried for 3 parallel tests.

4. Conclusion

In summary, we explored a nanomaterial/nucleic acid biointerface engineered design strategy for constructing programmed biosensors with tunable dynamic ranges and higher specificity. The interaction between aptamer probes and GO could be finely tuned by changing the terminal poly A sequence of aptamer probes, in turn to build aptasensors with different quantification ranges for detecting target molecules. No complex design of DNA probe structures and nanomaterials was needed. The dynamic range of aptasensors could be tuned (from 2 ~500 μM to750 ~3500 μM) and broadened (to 3 orders) by singly or combined using different aptamer probes. The aptasensors accommodated accurate analysis of ATP in serum and milk, and could be applied to detect microorganism contaminations. This work demonstrates how the biointerface between nanomaterials and recognition biomolecules could be designed to construct

View Article Online
DOI: 10.1039/C9TB02388G

programmed biosensors, and may provide a general biosensing platform for analyzing important analytes in medical, food safety and environment areas by using different aptamers.

Conflicts of interest

There are no conflicts to declare.

Acknowledgements

This work was financially supported by National Natural Science Foundation of China (No. 21804095, No. 21621003, No. 21235004, No. 21327806), China Postdoctoral Science Foundation (No. 2018M631079), the Fundamental Research Funds for the Central Universities (No. 2018SCU12048), National Key Research and Development Program of China (No. 2016YFA0203101), Tsinghua University Initiative Scientific Research Program.

References

1. N. Nakatsuka, K.-A. Yang, J. M. Abendroth, K. M. Cheung, X. Xu, H. Yang, C. Zhao, B. Zhu, Y. S. Rim, Y. Yang, P. S. Weiss, M. N. Stojanović and A. M. Andrews, *Science*, 2018, **362**, 319-324.
2. L. Zhang, S. Wan, Y. Jiang, Y. Wang, T. Fu, Q. Liu, Z. Cao, L. Qiu and W. Tan, *J. Am. Chem. Soc.*, 2017, **139**, 2532-2540.
3. M. R. Dunn, R. M. Jimenez and J. C. Chaput, *Nat. Rev. Chem.*, 2017, **1**, 0076.
4. J. Canoura, Z. Wang, H. Yu, O. Alkhamis, F. Fu and Y. Xiao, *J. Am. Chem. Soc.*, 2018, **140**, 9961-9971.
5. Y. Li, X. Teng, K. Zhang, R. Deng and J. Li, *Anal. Chem.*, 2019, **91**, 3989-3996.

View Article Online
DOI: 10.1039/C9TB02388G

6. W. Chen, C. Yan, L. Cheng, L. Yao, F. Xue and J. Xu, *Biosens. Bioelectron.*, 2018, **117**, 845-851.

7. X. Zhang, C. Huang, Y. Jiang, Y. Jiang, J. Shen and E. Han, *J. Agric. Food Chem.*, 2018, **66**, 10106-10112.

8. X. Xia, H. Wang, H. Yang, S. Deng, R. Deng, Y. Dong and Q. He, *J. Agric. Food Chem.*, 2018, **66**, 12431-12438.

9. H. Yang, W. Zhao, S. Deng, K. Zhang, Z. Zhao, R. Deng, Q. He and J. Li, *ACS Applied Bio Materials*, 2019, DOI: 10.1021/acsabm.9b00738.

10. H. Pei, Y. Zheng, R. Kong, L. Xia and F. Qu, *Biosens. Bioelectron.*, 2016, **85**, 76-82.

11. S. Wu, L. Liu, N. Duan, Q. Li, Y. Zhou and Z. Wang, *J. Agric. Food Chem.*, 2018, **66**, 1949-1954.

12. X. Xia, Y. Wang, H. Yang, Y. Dong, K. Zhang, Y. Lu, R. Deng and Q. He, *Food Chem.*, 2019, **283**, 32-38.

13. R.-M. Kong, L. Ding, Z. Wang, J. You and F. Qu, *Anal. Bioanal. Chem.*, 2015, **407**, 369-377.

14. R.-M. Kong, X. Zhang, L. Ding, D. Yang and F. Qu, *Anal. Bioanal. Chem.*, 2017, **409**, 5757-5765.

15. L. Sheng, Y. Lu, S. Deng, X. Liao, K. Zhang, T. Ding, H. Gao, D. Liu, R. Deng and J. Li, *Chem. Commun.*, 2019, **55**, 10096-10099.

16. X. Chen, Y. Wang, Y. Zhang, Z. Chen, Y. Liu, Z. Li and J. Li, *Anal. Chem.*, 2014, **86**, 4278-4286.

View Article Online
DOI: 10.1039/C9TB02388G

17. X. Ren, K. Zhang, R. Deng and J. Li, *Chem*, 2019, **5**, 2571-2592.

18. H. Li, P. Dauphin-Ducharme, G. Ortega and K. W. Plaxco, *J. Am. Chem. Soc.*, 2017, **139**, 11207-11213.

19. R. Deng, Y. Dong, X. Xia, Y. Dai, K. Zhang, Q. He, W. Zeng, X. Ren and J. Li, *Anal. Chem.*, 2018, **90**, 14347-14354.

20. F. Ricci, A. Vallée-Bélisle, A. J. Simon, A. Porchetta and K. W. Plaxco, *Acc. Chem. Res.*, 2016, **49**, 1884-1892.

21. K. Zhang, H. Gao, R. Deng and J. Li, *Angew. Chem. Int. Edit.*, 2019, **58**, 4790-4799.

22. A. Vallée-Bélisle, F. Ricci and K. W. Plaxco, *J. Am. Chem. Soc.*, 2012, **134**, 2876-2879.

23. B. Wei, J. Zhang, X. Ou, X. Lou, F. Xia and A. Vallée-Bélisle, *Anal. Chem.*, 2018, **90**, 1506-1510.

24. C. Lu, Z. Huang, B. Liu, Y. Liu, Y. Ying and J. Liu, *Angew. Chem. Int. Edit.*, 2017, **56**, 6208-6212.

25. Y.-B. Luo, J.-S. Cheng, Q. Ma, Y.-Q. Feng and J.-H. Li, *Anal. Methods*, 2011, **3**, 92-98.

26. Y. Wang, Z. Li, J. Wang, J. Li and Y. Lin, *Trends Biotechnol.*, 2011, **29**, 205-212.

27. L. Tang, H. Chang, Y. Liu and J. Li, *Adv. Funct. Mater.*, 2012, **22**, 3083-3088.

28. L. Tang, Y. Wang and J. Li, *Chem. Soc. Rev.*, 2015, **44**, 6954-6980.

29. Z. Huang and J. Liu, *Langmuir*, 2018, **34**, 1171-1177.

30. Y. Wang, Z. Li, D. Hu, C.-T. Lin, J. Li and Y. Lin, *J. Am. Chem. Soc.*, 2010, **132**, 9274-9276.

31. Y. Wang, Z. Li, T. J. Weber, D. Hu, C.-T. Lin, J. Li and Y. Lin, *Anal. Chem.*, 2013, **85**, 6775-6782.

32. Y. Wang, L. Tang, Z. Li, Y. Lin and J. Li, *Nat. Protoc.*, 2014, **9**, 1944.

33. L. Tang, Y. Wang, Y. Liu and J. Li, *ACS Nano*, 2011, **5**, 3817-3822.

34. Y. Wang, Z. Li, M. Liu, J. Xu, D. Hu, Y. Lin and J. Li, *Anal. Chim. Acta.*, 2017, **983**, 1-8.

35. R. Deng, K. Zhang, L. Wang, X. Ren, Y. Sun and J. Li, *Chem*, 2018, **4**, 1373-1386.

36. H. Chang, L. Tang, Y. Wang, J. Jiang and J. Li, *Anal. Chem.*, 2010, **82**, 2341-2346.

37. L. Lin, Y. Liu, X. Zhao and J. Li, *Anal. Chem.*, 2011, **83**, 8396-8402.

38. X. Liu, Y. Li, J. Liang, W. Zhu, J. Xu, R. Su, L. Yuan and C. Sun, *Talanta*, 2016, **160**, 99-105.

39. J. N. Zadeh, C. D. Steenberg, J. S. Bois, B. R. Wolfe, M. B. Pierce, A. R. Khan, R. M. Dirks and N. A. Pierce, *J. Comput. Chem.*, 2011, **32**, 170-173.

40. S.-J. Chen, Y.-F. Huang, C.-C. Huang, K.-H. Lee, Z.-H. Lin and H.-T. Chang, *Biosens. Bioelectron.*, 2008, **23**, 1749-1753.

41. E. Babu, P. Muthu Mareeswaran, A. Ramdass, P. Ramesh and S. Rajagopal, *J. Lumin.*, 2016, **175**, 267-273.

42. J.-H. Park, J.-Y. Byun, W.-B. Shim, S. U. Kim and M.-G. Kim, *Biosens. Bioelectron.*, 2015, **73**, 26-31.